

Current-phase relation and flux-dependent thermoelectricity in Andreev interferometers

Pavel E. Dolgirev,¹ Mikhail S. Kalenkov,^{2,3} and Andrei D. Zaikin^{4,5}

¹*Skolkovo Institute of Science and Technology, Skolkovo Innovation Center, 3 Nobel St., 143026 Moscow, Russia*

²*I.E. Tamm Department of Theoretical Physics, P.N. Lebedev Physical Institute, 119991 Moscow, Russia*

³*Moscow Institute of Physics and Technology, Dolgoprudny, 141700 Moscow region, Russia*

⁴*Institut für Nanotechnologie, Karlsruher Institut für Technologie (KIT), 76021 Karlsruhe, Germany*

⁵*P.L. Kapitza Institute for Physical Problems, 119334 Moscow, Russia*

(Dated: June 7, 2021)

We predict a novel (I_0, ϕ_0) -junction state of multi-terminal Andreev interferometers that emerges from an interplay between long-range quantum coherence and non-equilibrium effects. Under non-zero bias V the current-phase relation $I_S(\phi)$ resembles that of a ϕ_0 -junction differing from the latter due to a non-zero average $I_0(V) = \langle I_S(\phi) \rangle_\phi$. The flux-dependent thermopower $\mathcal{S}(\Phi)$ of the system exhibits features similar to those of a (I_0, ϕ_0) -junction and in certain limits it can reduce to either odd or even function of Φ in the agreement with a number of experimental observations.

I. INTRODUCTION

Multi-terminal heterostructures composed of interconnected superconducting (S) and normal (N) terminals (frequently called Andreev interferometers) are known to exhibit non-trivial behavior provided the quasiparticle distribution function inside the system is driven out of equilibrium. For instance, it was demonstrated both theoretically^{1–3} and experimentally⁴ that biasing two N-terminals in a four-terminal NS configuration by an external voltage V one can control both the magnitude and the phase dependence of the supercurrent flowing between two S-terminals and – in particular – provide switching between zero- and π -junction states at certain values of V . In other words, a π -junction state in SNS structures can be induced simply by driving electrons in the N-metal out of equilibrium.

Another way to generate non-equilibrium electron states in Andreev interferometers is to expose the system to a temperature gradient. As a result, an electric current (and/or voltage) response occurs in the system which is the essence of the thermoelectric effect⁵. Usually the magnitude of this effect in both normal metals and superconductors is small in the ratio between temperature and the Fermi energy $T/\varepsilon_F \ll 1$, however, it can increase dramatically in the presence of electron-hole asymmetry. The symmetry between electrons and holes in superconducting structures can be lifted for a number of reasons, such as, e.g., spin-dependent electron scattering (for instance, at magnetic impurities⁶, spin-active interfaces⁷ or superconductor-ferromagnet boundaries⁸) or Andreev reflection at different NS-interfaces in an SNS structure with a non-zero phase difference between two superconductors^{9,10} (see also¹¹). The latter mechanism could be responsible for large thermoelectric signal observed in various types of Andreev interferometers^{12–16}.

Yet another important feature of some of the above observations is that the detected thermopower was found to oscillate as a function of the applied magnetic flux Φ with the period equal to the flux quantum $\Phi_0 = \pi c/e$,

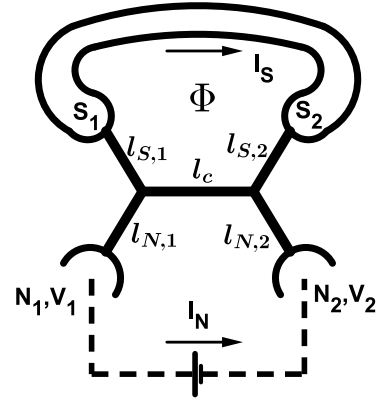


FIG. 1: A four-terminal structure consisting of five diffusive normal wires of lengths l_c , $l_{N,1,2}$ and $l_{S,1,2}$ and cross sections \mathcal{A}_c , $\mathcal{A}_{N,1,2}$ and $\mathcal{A}_{S,1,2}$ connecting two normal terminals biased with a constant voltage $V = V_2 - V_1$ and two superconducting terminals embedded in a superconducting loop encircling the magnetic flux Φ . We also indicate the currents I_S and I_N flowing respectively in superconducting and normal contours of our setup.

thus indicating that the thermoelectric effect essentially depends on the phase of electrons in the interferometer. The symmetry of such thermopower oscillations was observed to be either odd or even in Φ depending on the sample topology¹². Also, with increasing bias voltage these oscillations were found to vanish and then re-appear at yet higher voltages with the phase shifted by π ¹⁴. Despite subsequent attempts to attribute the results¹² to charge imbalance effects¹⁷ or mesoscopic fluctuations¹⁸ no unified and consistent explanation for the observations^{12–16} has been offered so far.

In this paper we address the properties of SNS junctions embedded in multi-terminal configurations with both bias voltage and thermal gradient applied to different normal terminals. For the configuration depicted in Fig. 1 we will demonstrate that at low enough tem-

peratures and with no thermal gradient the corresponding SNS structure exhibits characteristic features of what we will denote as (I_0, ϕ_0) -junction state: The current I_S flowing through the superconducting contour of our setup (as shown in Fig. 1) is predicted to have the form

$$I_S = I_0(V) + I_1(V, \phi + \phi_0(V)), \quad (1)$$

where $I_0 = \langle I_S \rangle_\phi$ and $I_1(V, \phi)$ is a 2π -periodic function of the superconducting phase difference $\phi = 2\pi\Phi/\Phi_0$ across our SNS junction. At zero bias $V \rightarrow 0$ both I_0 and ϕ_0 vanish and the term I_1 reduces to the equilibrium supercurrent in diffusive SNS structures^{19,20}. At low enough V the contribution I_1 essentially coincides with the voltage-controlled Josephson current² (with ϕ_0 jumping from 0 to π with increasing V), while at higher voltages with a good accuracy we have $I_1 \simeq \tilde{I}_C(V) \sin(\phi + \phi_0)$ with non-zero phase shift $\phi_0(V)$ which tends to $\pi/2$ in the limit of large V . This behavior resembles that of an equilibrium ϕ_0 -junction which develops nonvanishing supercurrent at $\phi = 0$. In contrast to the latter situation, however, here we drive electrons out of equilibrium, thereby generating extra current $I_0(V)$ along with the phase shift $\phi_0(V)$. Remarkably, also a thermoelectric signal does not vanish at $\phi = 0$ for non-zero V , as it will be demonstrated below.

The article is organized as follows. In Section II we briefly describe the quasiclassical Green function formalism employed in our further analysis. The general current-phase relation for our Andreev interferometer summarized in Eq. (1) is derived and analyzed in Section III. In Section IV we elaborate on the implications of this relation for the flux-dependent thermopower in multi-terminal Andreev interometers thereby proposing an interpretation for long-standing experimental puzzles^{12,14}. We close with a brief summary of our key observations in Section V.

II. QUASICLASSICAL FORMALISM

In what follows we will employ the quasiclassical Usadel equations which can be written in the form²¹

$$iD\nabla(\tilde{G}\nabla\tilde{G}) = [\hat{1} \otimes \hat{\Omega} + eV(\mathbf{r}), \tilde{G}], \quad \tilde{G}^2 = 1. \quad (2)$$

Here 4×4 matrix \tilde{G} represent the Green function in the Keldysh-Nambu space

$$\tilde{G} = \begin{pmatrix} \hat{G}^R & \hat{G}^K \\ 0 & \hat{G}^A \end{pmatrix}, \quad \hat{\Omega} = \begin{pmatrix} \varepsilon & \Delta(\mathbf{r}) \\ -\Delta^*(\mathbf{r}) & -\varepsilon \end{pmatrix}, \quad (3)$$

D is the diffusion constant, $V(\mathbf{r})$ is the electric potential, ε is the quasiparticle energy, $\Delta(\mathbf{r})$ is the superconducting order parameter equal to $|\Delta| \exp(i\phi_{1(2)})$ in the first (second) S-terminal and to zero otherwise. The retarded, advanced, and Keldysh components of the matrix \tilde{G} are 2×2 matrices in the Nambu space

$$\hat{G}^{R,A} = \begin{pmatrix} G^{R,A} & F^{R,A} \\ \tilde{F}^{R,A} & -G^{R,A} \end{pmatrix}, \quad \hat{G}^K = \hat{G}^R \hat{f} - \hat{f} \hat{G}^A, \quad (4)$$

where $\hat{f} = f_L \hat{1} + f_T \hat{\tau}_3$ is the distribution function matrix and $\hat{\tau}_3$ is the Pauli matrix. The current density \mathbf{j} is related to the matrix \tilde{G} by means of the formula

$$\mathbf{j} = -\frac{\sigma_N}{8e} \int \text{Tr}[\hat{\tau}_3(\tilde{G}\nabla\tilde{G})^K] d\varepsilon, \quad (5)$$

where σ_N is the Drude conductivity of a normal metal.

Resolving Usadel equations (2) for $\hat{G}^{R,A}$ in each of the normal wires, we evaluate both the spectral current and the kinetic coefficients²¹

$$\mathbf{j}_\varepsilon = \frac{1}{4} \text{Tr} \hat{\tau}_3 (\hat{G}^R \nabla \hat{G}^R - \hat{G}^A \nabla \hat{G}^A), \quad (6)$$

$$D_L = \frac{1}{2} - \frac{1}{4} \text{Tr} \hat{G}^R \hat{G}^A, \quad (7)$$

$$D_T = \frac{1}{2} - \frac{1}{4} \text{Tr} \hat{G}^R \hat{\tau}_3 \hat{G}^A \hat{\tau}_3, \quad (8)$$

$$\mathcal{Y} = \frac{1}{4} \text{Tr} \hat{G}^R \hat{\tau}_3 \hat{G}^A, \quad (9)$$

which enter the kinetic equations as

$$\nabla \mathbf{j}_L = 0, \quad \mathbf{j}_L = D_L \nabla f_L - \mathcal{Y} \nabla f_T + \mathbf{j}_\varepsilon f_T, \quad (10)$$

$$\nabla \mathbf{j}_T = 0, \quad \mathbf{j}_T = D_T \nabla f_T + \mathcal{Y} \nabla f_L + \mathbf{j}_\varepsilon f_L. \quad (11)$$

Equation (5) for the current density can then be cast to the form

$$\mathbf{j} = \frac{\sigma_N}{2e} \int \mathbf{j}_T d\varepsilon. \quad (12)$$

Analogously one can define the heat current density

$$\mathbf{j}_Q = \frac{\sigma_N}{2e^2} \int \mathbf{j}_L \varepsilon d\varepsilon. \quad (13)$$

Eqs. (2) should be supplemented by proper boundary conditions. Here we only address the limit of transparent interfaces and continuously match the normal wires Green functions \tilde{G} to those in the normal terminals

$$\hat{G}_{N_i}^R = -\hat{G}_{N_i}^A = \hat{\tau}_3, \quad (14)$$

$$f_{L/T, N_i} = \frac{1}{2} \left[\tanh \frac{\varepsilon + eV_i}{2T_i} \pm \tanh \frac{\varepsilon - eV_i}{2T_i} \right], \quad (15)$$

and in the superconducting ones

$$\hat{G}^{R,A} = \pm \frac{\begin{pmatrix} \varepsilon & \Delta \\ -\Delta^* & -\varepsilon \end{pmatrix}}{\sqrt{(\varepsilon \pm i\delta)^2 - \Delta^2}}, \quad (16)$$

$$\hat{G}^K = (\hat{G}^R - \hat{G}^A) \tanh \frac{\varepsilon}{2T}. \quad (17)$$

The spectral currents $\mathbf{j}_\varepsilon, \mathbf{j}_T, \mathbf{j}_L$ obey the Kirchhoff-like equations in all nodes of our structure.

III. (I_0, ϕ_0) -JUNCTION

We first consider a symmetric four-terminal setup of Fig. 1 with wire lengths $l_{S(N),1} = l_{S(N),2} = l_{S(N)}$,

equal cross sections $\mathcal{A}_{S(N),1} = \mathcal{A}_{S(N),2} = \mathcal{A}_c = \mathcal{A}$ and voltages²² $V_{1/2} = \mp V/2$. The spectral part of the Usadel equation (2) is solved numerically in a straightforward manner (cf, e.g., Ref. 2). This solution enables us to find the retarded and advanced Green functions $\hat{G}^{R,A}$ and to evaluate the spectral current j_ε (6) as well as the kinetic coefficients (7)-(9). In order to resolve the kinetic equations and to determine the current-phase relation for our setup we will adopt the following strategy. We first obtain a simple approximate analytic solution and then verify it by a rigorous numerical analysis.

Let us for a moment assume that the phase difference ϕ is small as compared to unity and relax this assumption in the very end of our calculation. In this case one can proceed perturbatively and resolve the kinetic equations in the first order in $j_\varepsilon \propto \phi$. Within the same accuracy, one can drop the small terms $\sim \mathcal{Y}$ and neglect the energy dependence of $D_L \approx 1$. With the aid of Eq. (12) we arrive at the expressions for the spectral currents $I_{S(N)}(\varepsilon) = \sigma_N j_T \mathcal{A} / (2e)$ flowing in the superconducting (normal) contours of our circuit²³, see Fig. 1. We obtain

$$I_S(\varepsilon) = \sigma_N f_L^0 j_\varepsilon \mathcal{A} / (2e) - f_T^0 \mathcal{R}_c^T / \mathcal{N} \quad (18)$$

$$I_N(\varepsilon) = -f_T^0 (\mathcal{R}_c^T + 2\mathcal{R}_S^T) / \mathcal{N}, \quad (19)$$

where we defined

$$\mathcal{N} = \mathcal{R}_c^T (\mathcal{R}_S^T + \mathcal{R}_N^T) + 2\mathcal{R}_S^T \mathcal{R}_N^T \quad (20)$$

and the spectral resistances $\mathcal{R}_i^T = (\mathcal{A}\sigma_N)^{-1} \int_{l_i} dx / D_{T,i}$ (which reduce to that for a normal wire of length l_i in the normal state with $D_T \equiv 1$). The distribution functions $f_{L/T}^0$ are given by Eq. (15) with $V_i \rightarrow V/2$ and $T_i \rightarrow T$. Integrating Eqs. (18) and (19) over energy ε we obtain approximate expressions for the currents I_N and I_S .

In addition to the above perturbative analysis we carried out a rigorous numerical calculation of both I_S and I_N involving no approximations. In the low temperature limit $T \rightarrow 0$ the corresponding results are displayed in Figs. 2 and 3 along with approximate results derived from Eqs. (18) and (19) in the same limit. It is satisfactory to observe that our simple perturbative procedure yields very accurate result for the current $I_N(\phi)$ not only for small phases but for all values of ϕ , see Fig. 2. This current is an even 2π -periodic function of ϕ and $\langle I_N \rangle_\phi \propto V$. Likewise, for the system under consideration we have $I_0 = \langle I_S \rangle_\phi \propto V$.

Below in this section we will mainly concentrate on the phase dependence of the current I_S . Fig. 3 demonstrates that – in the agreement with our expectations – our simple analytic result for $I_S(\phi)$ derived from Eq. (18) is quantitatively accurate at sufficiently small phase values or, more generally, at all phases ϕ in the vicinity of the points πn . Moreover, even away from these points Eq. (18) remains qualitatively correct capturing all essential features obtained within our rigorous numerical analysis. These considerations yield Eq. (1) which represents the first key result of our work.

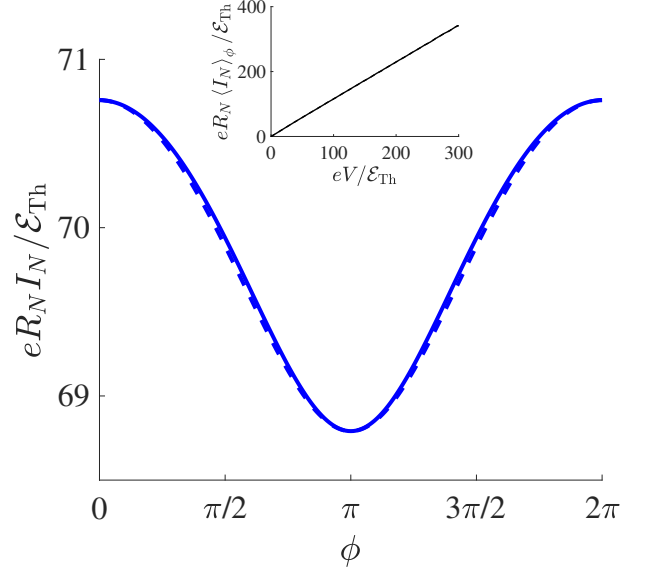


FIG. 2: (Color online) The phase dependence of the current I_N at $T \rightarrow 0$ for $eV = 60\varepsilon_{Th}$. Here we set $l_S = l_N = l_c$ and $\varepsilon_{Th} = 10^{-3}\Delta$. The result for $I_N(\phi)$ derived from an approximate Eq. (19) is indicated by the dashed line, the solid line correspond to our exact numerical solution. The inset illustrates $\langle I_N \rangle_\phi$ as a function of the voltage bias V .

It is instructive to analyze the above expressions in more details. The first term in the right-hand side of Eq. (18) is a familiar one. In equilibrium it accounts for dc Josephson current^{19,20}, while at non-zero bias V and in the limit $l_c \rightarrow 0$ (in which the last term in Eq. (18) vanishes) it reduces to the results^{2,3} demonstrating voltage-controlled $0-\pi$ transitions in SNS junctions. In contrast, the last term in Eq. (18) is a new one being responsible for both I_0 and ϕ_0 parts. This term is controlled by the combination $D_T(\phi)\nabla f_T$, where D_T is an even function of ϕ . Hence, the net current $I_S(\varepsilon)$ is no longer an odd function of ϕ .

The physics behind this result is transparent. In the presence of a non-zero bias V a dissipative current component, which we will further label as $I_d(V)$, is induced in the normal wire segments $l_{S,1}$ and $l_{S,2}$. At NS interfaces this current gets converted into extra (V -dependent) supercurrent flowing across a superconducting loop. Since at low temperatures and energies electrons in normal wires attached to a superconductor remain coherent keeping information about the phase ϕ , dissipative currents in such wires also become phase (or flux) dependent demonstrating even in ϕ Aharonov-Bohm-like (AB) oscillations^{24–27}, i.e. $I_d(V, \phi) = I_0(V) + I_{AB}(V, \phi)$, where $I_0(V) \propto V$. Combining this contribution to the current I_S with an (odd in ϕ) Josephson current $I_J(V, \phi)$ we immediately arrive at Eq. (1) with $I_1 = I_J + I_{AB}$.

The behavior of the phase shift $\phi_0(V)$ displayed in the inset of Fig. 3 is the result of a trade-off between Josephson and Aharonov-Bohm contributions to I_1 . At low bias voltages I_J dominates over I_{AB} , and we have $\phi_0 \approx 0$. In-

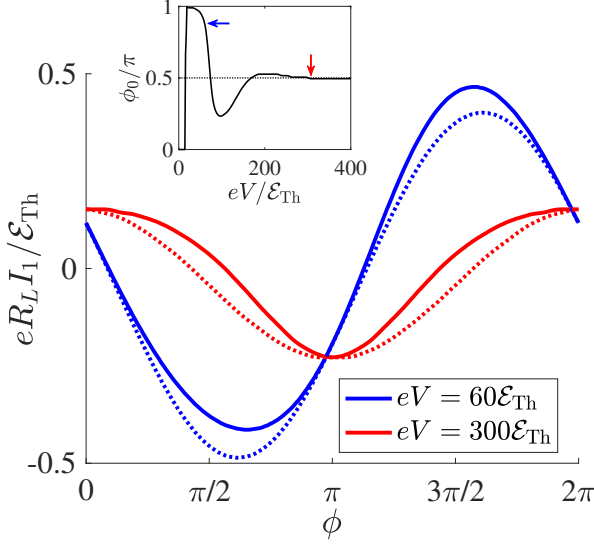


FIG. 3: (Color online) The phase dependence of the current I_1 at $T \rightarrow 0$ for $eV = 60\mathcal{E}_{Th}$ and $eV = 300\mathcal{E}_{Th}$. Solid lines indicate our exact numerical solution. Dotted lines correspond to a simple analytic expression for $I_1(\phi)$ derived from Eq. (18). The parameters are the same as in Fig. 2. Inset: The phase shift ϕ_0 as a function of V . Arrows indicate the voltage values $eV = 60\mathcal{E}_{Th}$ and $eV = 300\mathcal{E}_{Th}$.

creasing the bias to values $eV \sim 20\mathcal{E}_{Th}$, in full agreement with previous results² we observe the transition to the π -junction state implying the sign change of I_J . Here we defined the Thouless energy $\mathcal{E}_{Th} = D/L^2 \ll \Delta$, where $L = 2l_S + l_c$ is the total length of three wire segments between two S-terminals (see Fig. 1). At even higher bias voltages both terms I_J and I_{AB} eventually become of the same order. For $v = (eV/2\mathcal{E}_{Th})^{1/2} \gg 1$ and at $T \ll \mathcal{E}_{Th}$ we have² $I_J = I_C(V) \sin \phi$, where for our geometry

$$I_C(V) \simeq \frac{128(1+v^{-1})}{9(3+2\sqrt{2})} \frac{V}{R_L} e^{-v} \sin(v+v^{-1}). \quad (21)$$

We also approximate²⁸ $I_{AB} \approx I_m \cos \phi$, where $I_m \approx 0.18\mathcal{E}_{Th}/eR_L$ and R_L is the normal resistance of the wire with length L . Hence, for $eV \gg \mathcal{E}_{Th} \gg T$ we obtain

$$I_1 \approx \sqrt{I_C^2 + I_m^2} \sin(\phi + \phi_0), \quad \phi_0(V) = \arctan \frac{I_m}{I_C(V)}.$$

The function $\phi_0(V)$ (restricted to the interval $0 \leq \phi_0 \leq \pi$) shows damped oscillations and saturates to the value $\phi = \pi/2$ in the limit of large V , as it is also illustrated in the inset of Fig. 3.

At higher $T > \mathcal{E}_{Th}$ the Josephson current decays exponentially with increasing T whereas the Aharonov-Bohm term shows a much weaker power-law dependence^{26,27} $I_{AB} \propto 1/T$, thus dominating the expression for I_1 and implying that $\phi_0 \simeq \pi/2$ at such values of T .

For completeness, we point out that a (I_0, ϕ_0) -junction state is also realized in a cross-like geometry with $l_c = 0$

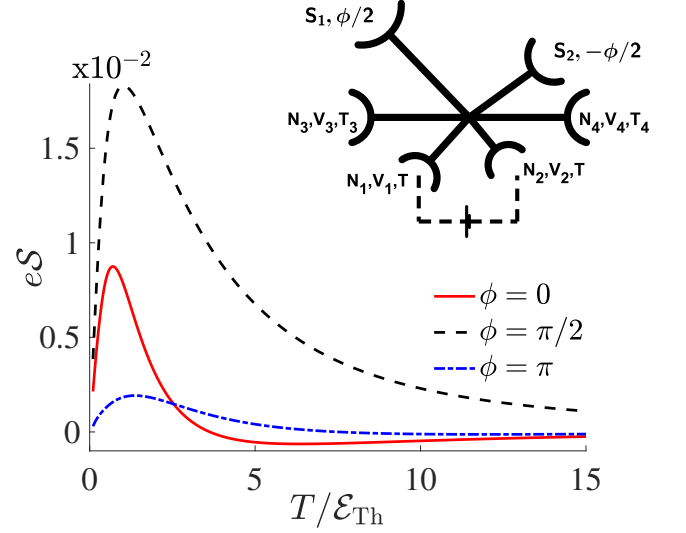


FIG. 4: (Color online) The temperature dependence of the thermopower $\mathcal{S} = V_T/\delta T$ between the terminals N_3 and N_4 of the six-terminal setup schematically illustrated in the inset. Different curves correspond to different values of ϕ . Here we set $eV = 0.9\Delta$, $\mathcal{E}_{Th} = 10^{-2}\Delta$ and fix the wire lengths as $l_{S,1} = 0.2L$, $l_{S,2} = 0.8L$, $l_{N,1} = 0.3L$, $l_{N,2} = 0.7L$ and $l_{N,3} = l_{N,4} = 0.5L$.

provided we set $l_{S,1} \neq l_{S,2}$ and $l_{N,1} \neq l_{N,2}$ (see, e.g., Fig. 4 below). Under these conditions the distribution function f_T at the wire crossing point differs from zero resulting in a non-vanishing even in ϕ contribution to I_S containing $D_T(\phi)\nabla f_T$. However, if either $l_{S,1} = l_{S,2}$ or $l_{N,1} = l_{N,2}$ this even in ϕ contribution vanishes and we get back to the results^{2,3} describing 0- and π -junction states.

IV. FLUX-DEPENDENT THERMOPOWER

We now turn to the thermoelectric effect. It was argued⁹⁻¹¹ that in Andreev interferometers this effect may become large provided the phase difference ϕ between superconducting electrodes differs from πn . Below we will demonstrate that a large thermopower can be induced by a temperature gradient even if $\phi = 0$.

To this end let us somewhat modify the setup in Fig. 1 by setting $l_c = 0$ and attaching two extra normal terminals N_3 and N_4 as shown in Fig. 4. These terminals are disconnected from the external circuit and are maintained at different temperatures T_3 and T_4 , while the temperature of the remaining four terminals equals to T .

We first set $\phi = 0$ and evaluate the thermoelectric voltage $V_T = V_3 - V_4$ between N_3 and N_4 induced by a thermal gradient $\delta T = T_3 - T_4$. For simplicity, below we consider the configuration with $l_{N,3} = l_{N,4}$. As no current

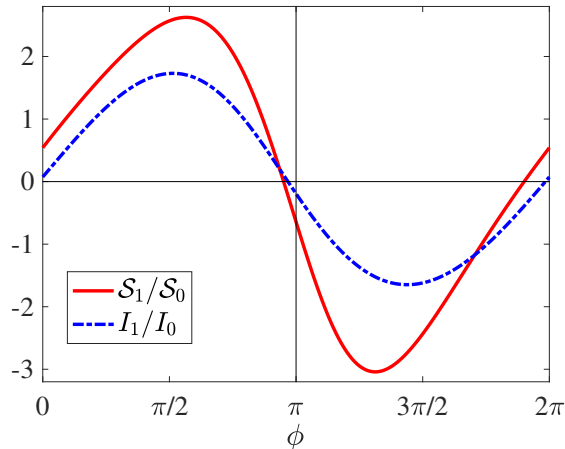


FIG. 5: (Color online) Thermopower \mathcal{S} and current I_S as functions of ϕ evaluated numerically for the six-terminal setup of Fig. 4 at $T = \mathcal{E}_{\text{Th}}$. The parameters are the same as in Fig. 4.

can flow into the terminals N_3 and N_4 , we obtain

$$\int \mathcal{G}_N^T(\varepsilon) [f_{T,N_3} - f_{T,N_4}] d\varepsilon = 0, \quad (22)$$

where $\mathcal{G}_N^T = 1/\mathcal{R}_{N_3}^T = 1/\mathcal{R}_{N_4}^T$ is the spectral conductance. Eq. (22) defines the relation between T_3 , T_4 and the induced voltages V_3 , V_4 . In the first order in $\delta T/T$ it yields the thermoelectric voltage in the form

$$eV_T = \frac{\delta T}{T} \frac{\int \frac{(\varepsilon + eV_N) \mathcal{G}_N^T(\varepsilon) d\varepsilon}{\cosh^2[(\varepsilon + eV_N)/(2T)]}}{\int \frac{\mathcal{G}_N^T(\varepsilon) d\varepsilon}{\cosh^2[(\varepsilon + eV_N)/(2T)]}}. \quad (23)$$

Here $V_N(V)$ is the induced electric potential of the terminals N_3 and N_4 evaluated at $\delta T = 0$. For any nonzero bias V the voltage V_N differs from zero as long as $l_{N,1} \neq l_{N,2}$. In this case the thermovoltage V_T (23) also remains nonzero as the spectral conductance \mathcal{G}_N^T explicitly depends on energy ε due to the superconducting proximity effect. On the other hand, in the absence of superconductivity the latter dependence disappears and the expression (23) vanishes identically even for nonzero V_N . This observation emphasizes a non-trivial interplay between superconductivity, quantum coherence and thermoelectricity in hybrid metallic nanostructures.

In order to recover the phase dependence of the thermoelectric voltage we treated the problem numerically. The corresponding results are displayed in Figs. 4 and 5. Fig. 4 demonstrates the temperature dependence of the thermopower $\mathcal{S} = V_T/\delta T$ at different values of ϕ . In Fig. 5 we present the thermopower as a function of ϕ at $T = \mathcal{E}_{\text{Th}}$ together with the current-phase relation $I_S(\phi)$ evaluated for the same setup. We observe that both functions $\mathcal{S}(\phi)$ and $I_S(\phi)$ demonstrate essentially the same

behavior and, hence, in complete analogy with Eq. (1) we have

$$\mathcal{S} = \mathcal{S}_0(V) + \mathcal{S}_1(V, \phi + \phi'_0(V)), \quad (24)$$

where $\mathcal{S}_0 = \langle \mathcal{S}(\phi) \rangle_\phi$ and $\mathcal{S}_1(V, \phi)$ is a 2π -periodic function of ϕ , which at high enough voltages only slightly deviates from a simple form $\mathcal{S}_1(V, \phi) \propto \sin \phi$ (cf. Fig. 5).

Eqs. (23), (24) represent the second key result of our work. It allows to conclude that in general the periodic dependence of the thermopower \mathcal{S} on the magnetic flux in Andreev interferometers is neither even nor odd in Φ , but it can reduce to either one of them depending on the system topology or, more specifically, on the relation between eV , T and the relevant Thouless energy \mathcal{E}_{Th} . The phase shift $\phi'_0(V)$ in Eq. (24) is not strictly identical to $\phi_0(V)$ in Eq. (1)²⁹, however, both these functions behave similarly. In fact, ϕ'_0 only slightly deviates from ϕ_0 (cf., e.g. Fig. 5). With increasing V , the phase ϕ'_0 also experiences an abrupt transition from 0 to π and then tends to $\pi/2$ in the limit of large voltages and/or temperatures.

Our findings allow to naturally interpret the experimental results¹² where both odd and even dependencies of V_T on Φ were detected depending on the system topology. Indeed, while at small enough eV and T we have $\phi'_0 \approx 0$ and $\mathcal{S}(\phi)$ remains an odd function, at larger voltages $eV \gtrsim 200\mathcal{E}_{\text{Th}}$ and/or temperatures $T \gg \mathcal{E}_{\text{Th}}$ the phase shift approaches $\phi'_0 \simeq \pi/2$ and the flux dependence of the thermopower $\mathcal{S}(\phi)$ (24) turns even, just as it was observed for some of the structures¹². Furthermore, as we already discussed, with increasing bias V the phase ϕ'_0 jumps from 0 to π which is fully consistent with the observations¹⁴. Thus, we believe the $0 - \pi$ transition for the flux-dependent thermopower $\mathcal{S}(\phi)$ detected in experiments¹⁴ has the same physical origin as that predicted¹⁻³ and observed⁴ earlier for dc Josephson current.

V. SUMMARY

In this work we have elucidated a non-trivial interplay between proximity-induced quantum coherence and non-equilibrium effects in multi-terminal hybrid normal-superconducting nanostructures. We have demonstrated that applying an external bias one drives the system to a (I_0, ϕ_0) -junction state in Eq. (1) determined by a trade-off between non-equilibrium Josephson and Aharonov-Bohm-like contributions. We have also analyzed the phase-coherent thermopower in such nanostructures which exhibits periodic dependence on the magnetic flux being in general neither even nor odd in Φ . Our results allow to formulate a clear physical picture explaining a number of existing experimental observations and calling for further experimental analysis of the issue.

Acknowledgements

We would like to thank A.G. Semenov for fruitful discussions. This work is a part of joint Russian-Greek Projects No. RFMEF161717X0001 and No. T4ΔPΩ-00031 Experimental and theoretical studies of physical

properties of low-dimensional quantum nanoelectronic systems. One of us (P.E.D.) also acknowledges support by Skoltech as a part of Skoltech NGP program and the hospitality of KIT during November 2017.

-
- ¹ A.F. Volkov, Phys. Rev. Lett. **74**, 4730 (1995).
 - ² F.K. Wilhelm, G. Schön, and A.D. Zaikin, Phys. Rev. Lett. **81**, 1682 (1998).
 - ³ S. Yip, Phys. Rev. B **58**, 5803 (1998).
 - ⁴ J.J.A. Baselmans, A.F. Morpurgo, B.J. van Wees and T. M. Klapwijk, Nature **397**, 43 (1999).
 - ⁵ See, e.g., V.L. Ginzburg, Rev. Mod. Phys. **76**, 981 (2004).
 - ⁶ M.S. Kalenkov, A.D. Zaikin, and L.S. Kuzmin, Phys. Rev. Lett. **109**, 147004 (2012).
 - ⁷ M.S. Kalenkov and A.D. Zaikin, Phys. Rev. B **91**, 064504 (2015).
 - ⁸ S. Kolenda, M.J. Wolf, and D. Beckmann, Phys. Rev. Lett. **116**, 097001 (2016).
 - ⁹ R. Seviour and A.F. Volkov, Phys. Rev. B **62**, R6116 (2000); V.R. Kogan, V.V. Pavlovskii, and A.F. Volkov, EPL **59**, 875 (2002); A.F. Volkov and V.V. Pavlovskii, Phys. Rev. B **72**, 014529 (2005).
 - ¹⁰ M.S. Kalenkov and A.D. Zaikin, Phys. Rev. B **95**, 024518 (2017).
 - ¹¹ P. Virtanen and T.T. Heikkilä, Phys. Rev. Lett. **92**, 177004 (2004); J. Low Temp. Phys. **136**, 401 (2004).
 - ¹² J. Eom, C.-J. Chien and V. Chandrasekhar, Phys. Rev. Lett. **81**, 437 (1998).
 - ¹³ D.A. Dikin, S. Jung, and V. Chandrasekhar, Phys. Rev. B **65**, 012511 (2001).
 - ¹⁴ A. Parsons, I.A. Sosnin, and V.T. Petrashov, Phys. Rev. B **67**, 140502(R) (2003).
 - ¹⁵ P. Cadden-Zimansky, Z. Jiang, and V. Chandrasekhar, New J. Phys. **9**, 116 (2007).
 - ¹⁶ C.D. Shelly, E.A. Matroзова, and V.T. Petrashov, Sci. Adv. **2**, 1501250 (2016).
 - ¹⁷ M. Titov, Phys. Rev. B **78**, 224521 (2008).
 - ¹⁸ P. Jacquod, and R.S. Whitney, EPL **91**, 67009 (2010).
 - ¹⁹ A.D. Zaikin and G.F. Zharkov, Fiz. Nizk. Temp. **7**, 375 (1981) [Sov. J. Low Temp. Phys. **7**, 181 (1981)].
 - ²⁰ P. Dubos, H. Courtois, B. Pannetier, F.K. Wilhelm, A.D. Zaikin, and G. Schön, Phys. Rev. B **63**, 064502 (2001).
 - ²¹ W. Belzig, F.K. Wilhelm, C. Bruder, G. Schön and A.D. Zaikin, Superlatt. Microstruct. **25**, 1251 (1999).
 - ²² For non-symmetric geometries the N-terminal potentials $V_{1,2}$ generally depend on ϕ .
 - ²³ As it is clear from Fig. 1, the superconducting contour (carrying the current I_S) includes the superconductor as well as the normal-wire segments $l_{S,1}$ and $l_{S,2}$, while the normal contour (with the current I_N) consists of the battery and the normal wire segments $l_{N,1}$ and $l_{N,2}$. The current through the normal-wire segment l_c obviously equals to $I_S + I_N$.
 - ²⁴ H. Nakano and H. Takayanagi, Solid State Commun. **80**, 997 (1991).
 - ²⁵ T.H. Stoof and Yu.V. Nazarov, Phys. Rev. B **54**, R772 (1996).
 - ²⁶ A.A. Golubov, F.K. Wilhelm, and A.D. Zaikin, Phys. Rev. B **55**, 1123 (1997).
 - ²⁷ H. Courtois, P. Gandit, D. Mailly, and B. Pannetier, Phys. Rev. Lett. **76**, 130 (1996).
 - ²⁸ Strictly speaking, the 2π -periodic even in ϕ function $I_{AB}(\phi)$ slightly deviates from a simple $\cos\phi$ -form, however, a small admixture of higher harmonics $\propto \cos(n\phi)$ with $n \geq 2$ does not alter any of our conclusions.
 - ²⁹ According to¹¹, the thermopower \mathcal{S} is determined by the derivative dI_S/dT . Hence, deviations between the phase shifts ϕ_0 and ϕ'_0 can be attributed to different temperature dependencies of Aharonov-Bohm I_{AB} and Josephson I_J contributions to I_1 . For completeness, we note that the derivative dI_N/dT in general also contributes to the thermopower.